Ziolkowski, Marek; Brauer, Hartmut:

Modelling of Seebeck effect in electron beam deep welding of dissimilar metals

URN: urn:nbn:de:gbv:ilm1-2014210107

Published OpenAccess: September 2014

Original published in:

Compel : international journal of computation & mathematics in electrical & electronic engineering. - Bradford : Emerald (ISSN-p 0332-1649). - 28 (2009) 1, S. 140-153.

DOI: 10.1108/03321640910918940

URL: http://dx.doi.org/10.1108/03321640910918940

[Visited: 2014-09-02]

COMPEL - The international journal for computation and mathematics in electrical and electronic engineering

Modelling of Seebeck effect in electron beam deep welding of dissimilar metals

Marek Ziolkowski Hartmut Brauer

Modelling of Seebeck effect in electron beam deep welding of dissimilar metals

Marek Ziolkowski
Department of Electromagnetic Fields/ThEE, Technische Universität Ilmenau, Ilmenau, Germany and Technical University of Szczecin, Szczecin, Poland, and
Hartmut Brauer
Department of Electromagnetic Fields/ThEE, Technische Universität Ilmenau, Ilmenau, Germany

Abstract

Purpose – The purpose of this paper is to present a 3D model of deep welding of dissimilar metals and to show how to model the electron beam deflection due to thermoelectric fields caused by temperature gradients in some dissimilar metals (Seebeck effect).

Design/methodology/approach – A 3D thermoelectric and heat conduction model is used to estimate the deflection of the electron beam used during welding of dissimilar metals. A weak coupling between analysed fields is assembled. Additionally, the influence of the deflection on the calculated fields was not taken into account. The problem is solved using a finite element method.

Findings – It is possible to model Seebeck effect in a relative simple way using the finite element approach.

Originality/value – The paper presents a detailed description of modelling procedure of a complex coupled field problem.

Keywords Electron beam welding, Finite element analysis, Metals, Electrical conductivity

Paper type Research paper

1. Introduction

The application of highly accelerated electrons as a tool for material processing in fusion, drilling and welding processes and also for surface treatment has been known since dozen years. The energy conversion in the workpiece indicates that the kinetic energy of the highly accelerated electrons is, at the operational point, not only converted into the heat necessary for welding, but is also released by heat radiation and heat dissipation (Figure 1(a)).

The high-energy density at the impact point causes the evaporation of the metal and thus allowing the following electrons a deeper penetration. This finally leads to a metal vapour cavity which is surrounded by a shell of fluid metal, covering the entire weld depth. This deep-weld effect allows nowadays penetration depths into steel materials of up to 300 mm. When a small diameter electron beam is used to create a long joint of two pieces, the beam axis must be in the same plane as the joint faces and aligned with the joint along its entire length. In the case of two dissimilar metals, even when the beam is properly aligned with the joint, magnetic forces can cause beam deflection, resulting in a significant loss of weld quality

COMPEL: The International Journal for Computation and Mathematics in Electrical and Electronic Engineering
Vol. 28 No. 1, 2009
pp. 140-153

0332-1649
DOI 10.1108/03321640910918940

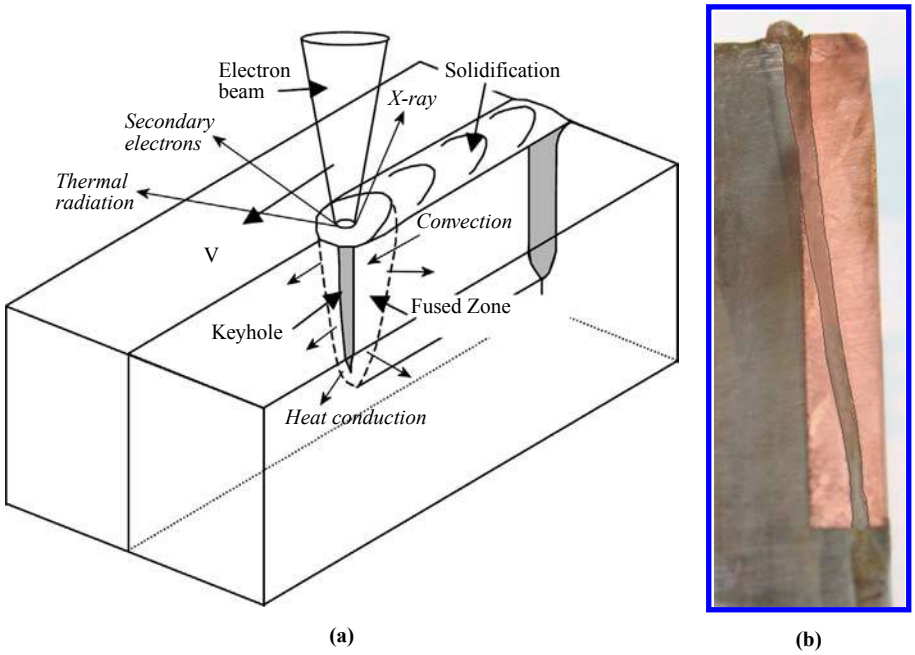

Figure 1.
Energy conversion during electron beam welding (a). Electron beam deflection in welding of two dissimilar metals (b)

(Figure 1(b)) (Nazarenko, 1982). One of the reasons of the electron beam deflection is due to thermoelectric fields caused by temperature gradients in some dissimilar metals (Seebeck effect (Shercliff, 1979)). Temperature gradients which exist between the top and bottom and in front of and behind the deep and narrow cavity produced by the electron beam near the joint plane cause thermoelectric currents flow in the workpiece. These currents induce magnetic field which deflects the electron beam, even when the beam from the electron gun is properly aligned with the joint. Interaction between the electron beam and the component of the magnetic field parallel to the welding direction deflects the electron beam in direction of the metal with a positive thermoelectric potential (Paulini *et al.*, 1990; Wei and Lii, 1990).

2. Seebeck effect

The Seebeck effect can be described by generalized Ohm's law as:

$$\mathbf{J} = \sigma\mathbf{E} - \sigma S\nabla T, \tag{1}$$

where $\mathbf{J}$ is a conduction current density vector, $\mathbf{E}$ is an electric field intensity vector, T denotes temperature, σ is an electrical conductivity, and S is called absolute thermoelectric power (Shercliff, 1979). Some data on the absolute thermoelectric power S of various metals are shown in Figure 2.

In the case of analysis of thermoelectric fields, the electric boundary conditions at interface between two media of different absolute thermoelectric power must be generalized and take the form:

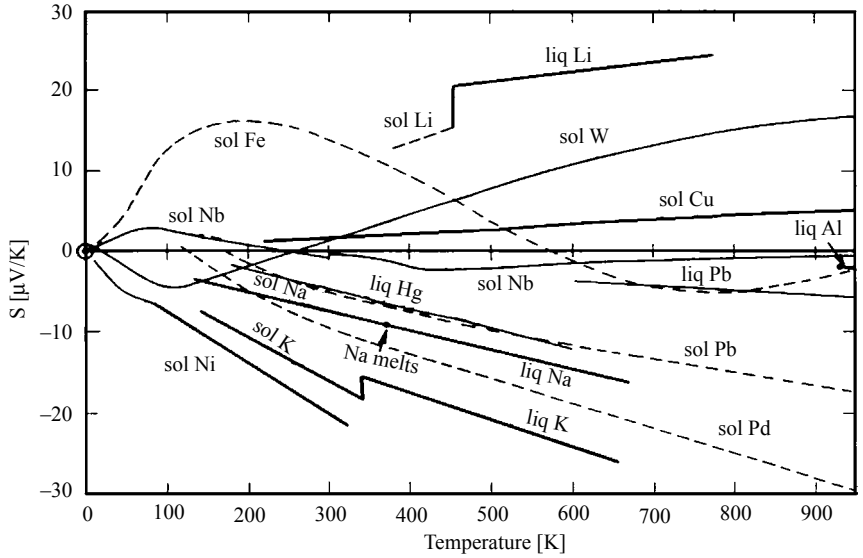

Figure 2.
Absolute thermoelectric power for pure metals

Source: Sherceliff (1979)

$$\frac{J_{s1}}{\sigma_1} - \frac{J_{s2}}{\sigma_2} = (S_2 - S_1)\frac{\partial T}{\partial s}, \quad J_{n1} = J_{n2}, \tag{2}$$

in which n and s denote normal and tangential components. Another boundary condition which is affected by the thermoelectricity is the thermal one which constrains temperature gradients normal to the interface:

$$k_1 \frac{\partial T_1}{\partial n} - k_2 \frac{\partial T_2}{\partial n} = (S_1 - S_2)TJ_n = (\Pi_1 - \Pi_2)J_n, \tag{3}$$

where k_i and Π_i are the thermal conductivity and Peltier coefficient, respectively. In equations (2) and (3), the contact resistance τ is neglected ($\tau = 0$). The term $(\Pi_1\text{-}\Pi_2)J_n$ describes the Peltier effect (thermoelectric cooling), which arises because the ability of the current to transport heat changes abruptly at the interface. Since the current must be continuous across the interface, the associated heat flow develops a discontinuity if Π_1 and Π_2 are different. This causes heat accumulation or depletion at the interface, depending on the sign of the current.

3. Solution strategy

In the presented paper, we use a 3D thermoelectric and heat conduction model to estimate the deflection of the electron beam used during welding of dissimilar metals. We assume a weak coupling, i.e. the coupling between analysed fields is sequentially ordered which means that the next calculated field does not have influence on the previous one. Additionally, we assume that the deflection does not influence calculated fields, i.e. the deflection is reasonably small. The analysis is split into four following steps:

(1) heat transfer (HT) problem, where the temperature field distribution is calculated;
(2) conductive media problem, where the current density distribution evoked by Seebeck effect is estimated;
(3) magnetic problem, where the magnetic flux density distribution produced by current density distribution calculated in the previous step is calculated; and
(4) deflection estimation, where the trajectory of the electron beam affected by previously calculated magnetic field is found.

Problems 1-3 are solved using a finite element method (FEM). In that case, we have applied the program COMSOL v.3.3 which enables to solve coupled problems using the same geometry model and can be easy coupled with Matlab. To solve problem 4, we wrote a small procedure in Matlab which simulates the deflection of the electron beam using a magnetic flux density calculated in FEM program.

4. Heat transfer model

During the welding process, the electron-beam moves along the weld joint. This movement requires a fairly complex model if we want to model the electron-beam as a moving heat source. In the presented analysis, we use a moving coordinate system which is fixed at the electron-beam axis and the workpiece is moving in the opposite direction of x-axis. Performing the coordinate trans-formation, the HT problem becomes a stationary convection-conduction problem which is much easier to model. The model includes some simplifications, e.g. dimensions of the model are finite although the transformation demands them infinitely long. It means that the analysis does not take into account effects near the start and end of the workpiece. The model does also not include the stirring process in the fused zone, which is very complex due to phase changes and material flow. The model geometry used in the simulations is shown in Figure 3.

The following equation describes HT in the workpiece:

$$\nabla \cdot (-k\nabla T) = Q_v - \rho C_p \mathbf{u} \cdot \nabla T, \tag{4}$$

where k is thermal conductivity, ρ is the density, C_p is specific heat capacity, $\mathbf{u}$ is the velocity vector, and Q_v denotes a volumetric heat source. The volumetric heat source is modelled as a conical distribution of power density which has a Gaussian distribution radially and a linear distribution axially (Goldak and Akhlaghi, 2005) and has the following form:

$$Q_v = Q_0\left[1 + (1-d)\frac{z}{h}\right]e^{-3(r/r_0)^2}, \quad r_0 = \frac{r_e - (r_e - r_i)(h+z)}{h}, \tag{5}$$

where Q_0 is the maximum value of heat intensity, r_e, r_i, h are dimensions of the keyhole (Figure 3(b)), and d is a parameter which determines the axial distribution of Q_v ($d = 0$ linear function, $d = 1$ constant function).

The maximum heat intensity Q_0 can be determined from the absorbed electron-beam power P using thermal energy conservation law:

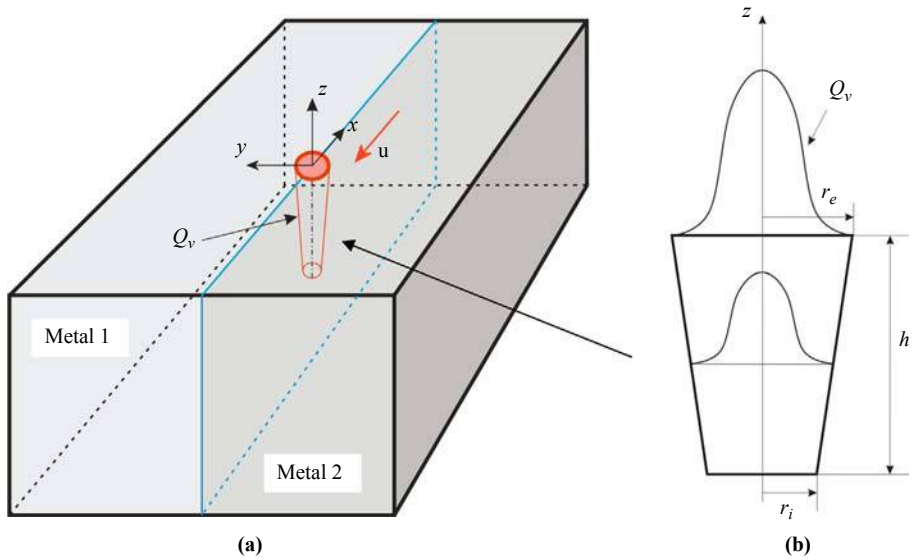

Figure 3.
Model of deep electron beam welding (a). 3D conical Gaussian heat source (b)

$$P = \int_V Q_v \mathrm{d}V = \int_{-h}^{0}\int_{0}^{2\pi}\int_{0}^{r_0} Q_v(r,z) r \mathrm{d}r\mathrm{d}\varphi\mathrm{d}z. \tag{6}$$

The final expression of Q_0 takes the form:

$$Q_0 = \frac{36P}{\pi(1-e^{-3})h} \quad \frac{1}{4(r_e^2 + r_e r_i + r_i^2) - (1-d)(3r_e^2 + 2r_e r_i + r_i^2)}. \tag{7}$$

Assuming $r_e = r_i = r_0$ and $1 - e^{-3} \cong 1$, we can write equation (5) in the following form:

$$Q_v(r,z) = \frac{6P}{\pi r_0^2 h} \frac{1 + (1-d)z/h}{1+d} e^{-3(r/r_0)^2}. \tag{8}$$

Additionally, the following boundary conditions have to be set on the boundaries of the workpiece (Figure 3(a)):

- left and right walls: thermal insulation:

$$-\mathbf{n}\cdot(-k\nabla T + \rho C_p \mathbf{u} T) = 0;$$

- back wall: constant temperature T_0 which is equal to the ambient temperature ($T = T_0$);
- front wall: convective flux:

$$\mathbf{q}\cdot\mathbf{n} = (\rho C_p \mathbf{u} T)\cdot\mathbf{n}, \quad \mathbf{n}\cdot(-k\nabla T) = 0;$$

- downside and upside walls: they lose heat due to natural convection and surface-to-ambient radiation. The corresponding heat flux expressions are:

$$-\mathbf{n}\cdot(-k\nabla T+\rho C_p\mathbf{u}T)=h(T_0-T)+\varepsilon\sigma_{\mathrm{SB}}\left(T_0^4-T^4\right);$$

where ε is hemispherical emissitivity, σ_{SB} is Stefan-Boltzman constant, and h is HT coefficient for natural convection.

5. Conductive media model (DC)

Using identity $\nabla\cdot\mathbf{J}=0$ and electric potential definition $\mathbf{E}=-\nabla V$, we transform equation (1) to the following equation:

$$\nabla\cdot[\sigma(T)\nabla V]=\nabla\cdot\mathbf{J}_e,\quad \mathbf{J}_e=-\sigma(T)S\nabla T, \tag{9}$$

where T is temperature calculated in HT problem. Equation (9) should be solved in regions Metals 1 and 2 (Figure 3). Current density $\mathbf{J}_e$ is only defined in elements where temperature T is less than melting temperature (T_{melt}).

On the downside wall, we set potential $V=0$ and on all the others, we force an electric insulation boundary condition ($\nabla\cdot\mathbf{J}=0$). At the interface between metals only standard continuity condition $\mathbf{n}\cdot(J_1-J_2)=0$ is implemented.

6. Magnetic modelf

Magnetic flux density $\mathbf{B}$ is calculated with the help of magnetic vector potential $\mathbf{A}$ defined as: $\mathbf{B}=\nabla\times\mathbf{A}$, together with Coulomb's gauge $\nabla\cdot\mathbf{A}=0$ to assure uniqueness of potential $\mathbf{A}$. Using above and Maxwell equation $\nabla\times\mathbf{H}=\mathbf{J}$, we receive the following equation:

$$\nabla\times\left(\frac{1}{\mu}\nabla\times\mathbf{A}\right)=\mathbf{J}, \tag{10}$$

where $\mathbf{J}$ is the current density distribution calculated in DC problem and μ is a magnetic permeability of media. In magnetic model (MA) problem, the geometry of the model has to be changed by adding additional ambient regions above and below the workpiece (Figure 3) to enable setting proper boundary conditions for magnetic vector potential $\mathbf{A}$. On all side walls, the electric insulation boundary condition ($\mathbf{n}\times\mathbf{H}=0$) is set whereas, on other walls, the magnetic insulation boundary condition $\mathbf{n}\times\mathbf{A}=0$ is chosen. Magnetic permeability μ for both metals is set to μ_{o} because even if we have ferromagnetic materials, in most parts of regions where currents evoked by Seebeck effect are flowing, temperature is greater than the Curie temperature (T_{Curie}) above which ferromagnetic materials loose their magnetic features.

7. Deflection model

The electron beam trajectory is deflected by Lorentz force according to the equation:

$$m\frac{\mathrm{d}\mathbf{v}}{\mathrm{d}t}=-e\mathbf{v}\times\mathbf{B}, \tag{11}$$

where m is electron mass (kg), e is electron charge (C), and $\mathbf{v}$ is the velocity of electrons in the electron beam. Because the Lorentz force is perpendicular to the local velocity vector, the magnitude of $\mathbf{v}$ remains constant and could be easy calculated from energy conservation law as:

$$\mathrm{v}_0 = \sqrt{\frac{2eU}{m}}, \tag{12}$$

where U is accelerating voltage. Displacement $\mathbf{r}$ of the electron can be calculated in an iterative way using following sequence of formulas:

$$\Delta\mathbf{v} = -\frac{e}{m}\mathbf{v}\times\mathbf{B}\Delta t \rightarrow \mathbf{v}_i = \mathbf{v}_{i-1} + \Delta\mathbf{v}, \quad \Delta\mathbf{r}_i = \mathbf{v}_i\Delta t \rightarrow \mathbf{r}_i = \mathbf{r}_{i-1} + \Delta\mathbf{r}_i \tag{13}$$

where Δt is a small enough time step determined by the user. The deflection of the electron beam is calculated until the depth of the keyhole is reached.

8. Simulations

8.1 Material data

As Metals 1 and 2, pure iron and copper are chosen, respectively. The thermal conductivity k and the specific heat capacity C_p are defined as temperature dependent functions according (Lide, 2006) (Figure 4).

The electrical conductivity is also taken into account as a temperature dependent function (Lide, 2006) (Figure 5).

Other material parameters are presented in Table I.

8.2 Results

In all simulations, following parameters have been chosen: vector of welding speed $\mathrm{u} = -2.5\mathbf{e}_x$ mm/s,absorbed electron beam power $P = 30$ kW, radius of the keyhole $r_0 = 0.3$ mm, depth of the keyhole $h = 70$ mm.

Figure 6 shows temperature distribution at various cross-section planes (HT analysis).

To model Seebeck effect, we have applied two approaches:

(1) simplified HT-MA analysis, where $\mathbf{J}$ in equation (10) is defined directly as $\mathbf{J}_e$ in equation (9); and

(2) full HT-DC-MA analysis.

In the first approach, the continuity conditions at the interface between metals are not fulfilled. Figure 7 shows current density distributions for both approaches. Figure 8 shows magnetic flux density in the vicinity of fusion zone for MA and DC-MA analysis.

After calculations of magnetic flux density distributions, the trajectory of the electron beam has been estimated according to equation (13). We have also implemented the possibility of tilting the electron beam against the workpiece z-axis which enables us, in a simple way, to test the influence of the tilt angle on the trajectory behaviour.

However, both approaches calculate deflection in the proper direction (the electron beam is deflected towards material with the greater absolute thermoelectric power), we

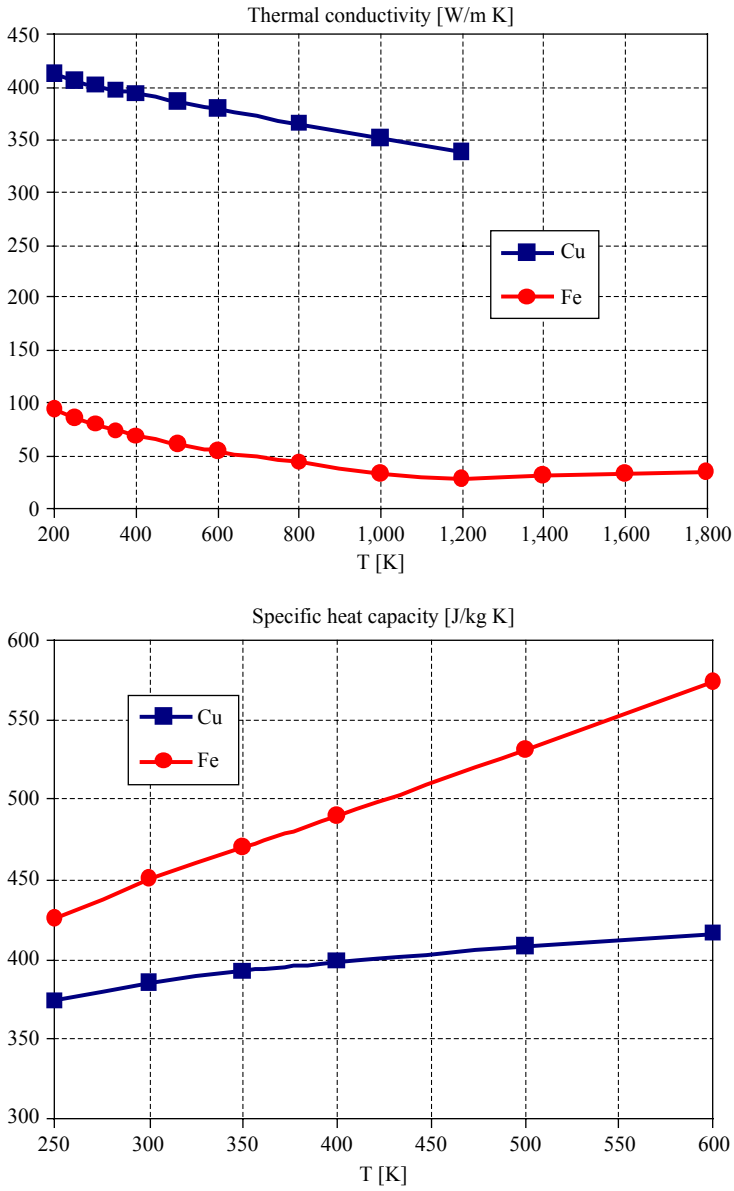

Source: Lide (2006)

Figure 4.
Thermal conductivity and specific heat capacity for pure iron and copper

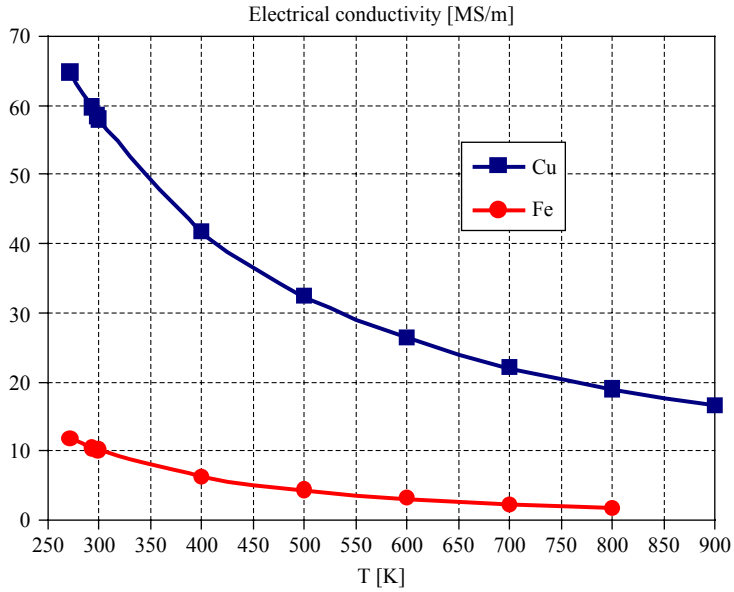

Figure 5.
Electrical conductivity of pure iron and copper

Source: Lide (2006)

	Fe	Cu
ρ (kg/m^3)	7,870	8,700
T_{melt} (K)	1,811	1,358
S_{800K} (μV/K)	−5.0	5.0
T_{Curie} (K)	1,043	–

Table I.
Parameters of materials used in simulations

can observe that in the case of HT-MA analysis the deflection of the electron beam is much stronger compared to HT-DC-MA analysis and the shape of the trajectory is far away from the observed trajectories in experiments (Figure 1(b)). Therefore, this kind of simplification should be avoided. Figure 9 shows trajectories of the electron beam for HT-MA analysis when the tilt angle is equal to 0° and 5°. The trajectory estimation procedure starts at $z = 5$ mm above the workpiece surface. In Figure 10, we present results of the trajectory estimation for HT-DC-MA analysis. In that case, trajectories shapes are more realistic. It was also possible to find the tilt angle which gives almost no deflection of the electron beam.

9. Conclusions

The presented analysis shows that it is possible to model Seebeck effect in a relative simple way using FEM. Further investigations should be done to implement the condition (2) into the analysis and also to study re-coupling of HT and DC analysis through the Peltier condition (3).

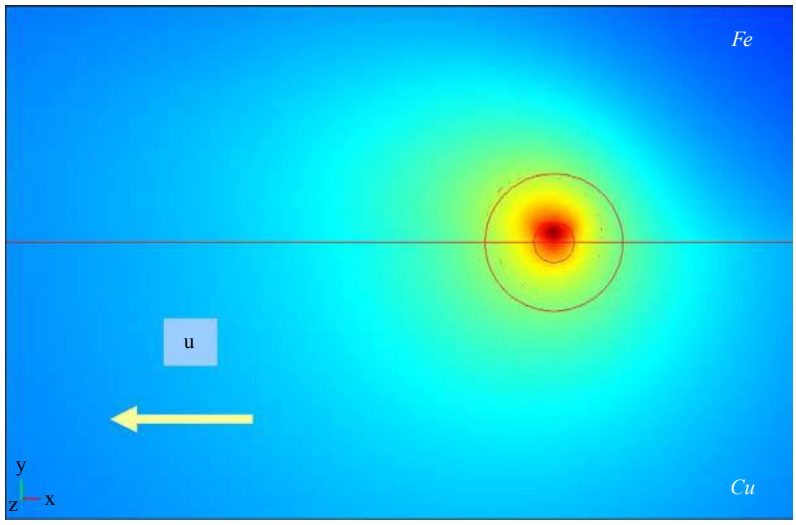

(a)

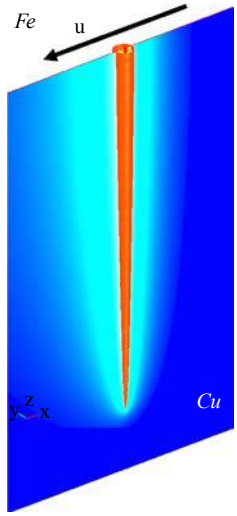

(b)

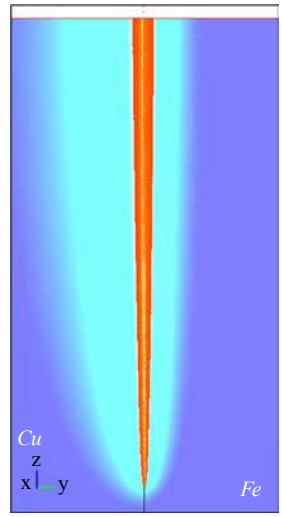

(c)

Figure 6.
Temperature distribution in the vicinity of the fused zone: (a) plane XY, $z = 0$; (b) XYZ view, $y = 0$; (c) plane YZ, $x = 0$

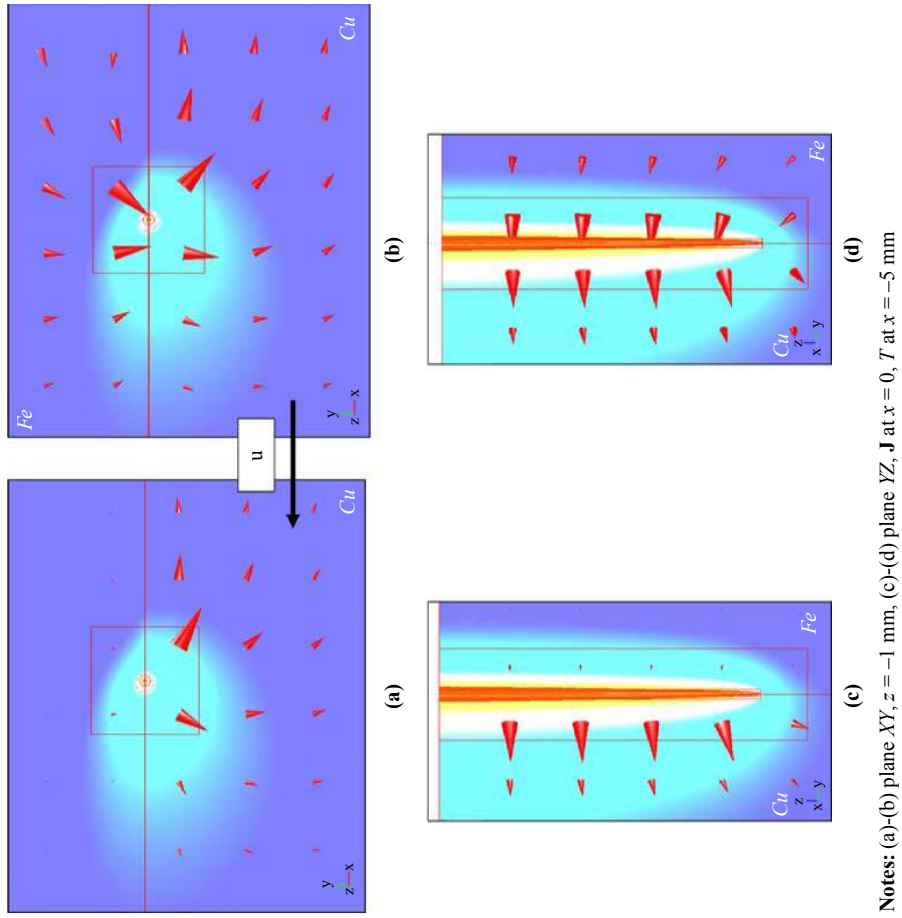

Figure 7.
Current density vectors together with temperature field distribution in the vicinity of the keyhole for HT-MA (a, c) and HT-DC-MA; (b, d) analysis

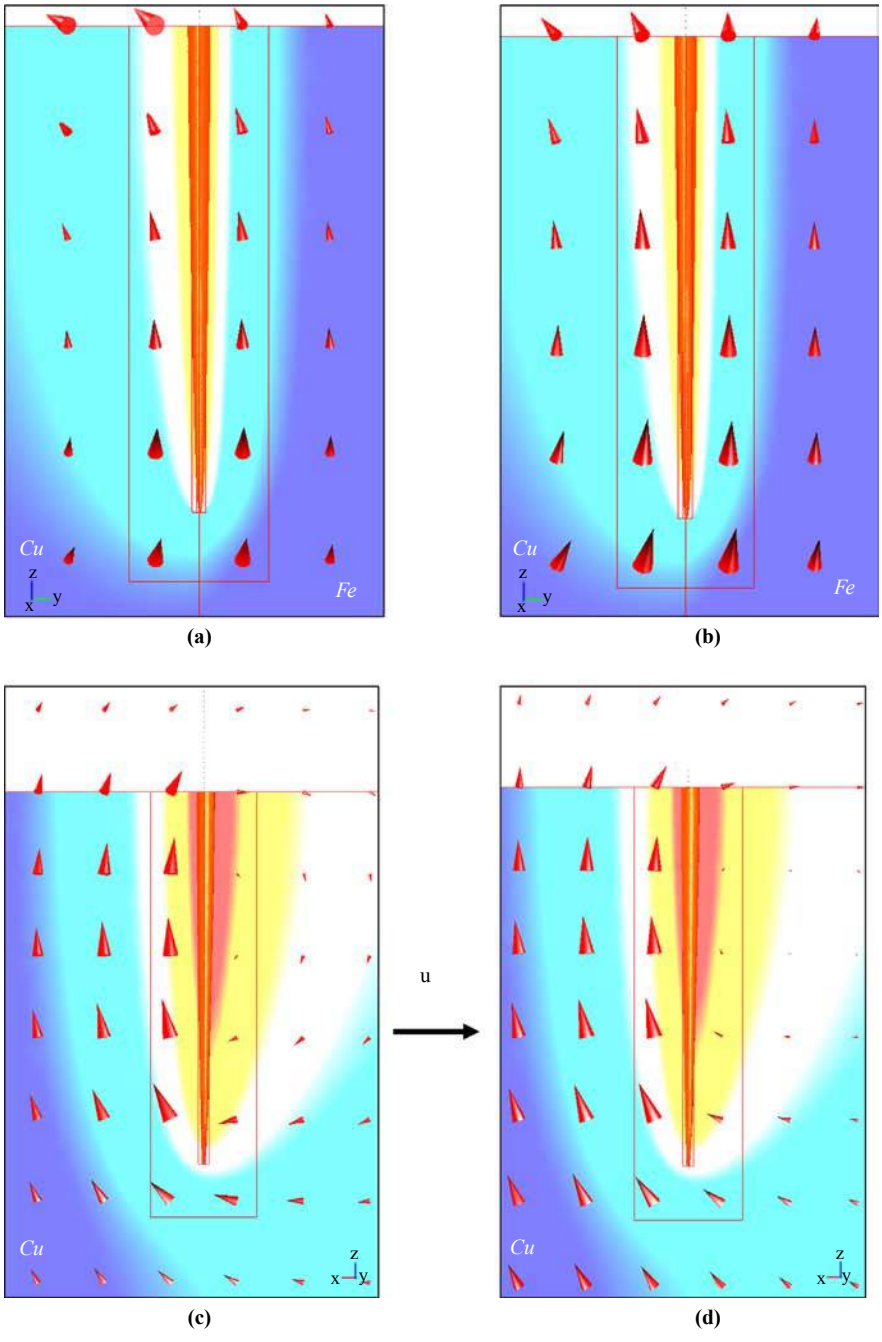

Notes: (a)-(b) plane *YZ*, **B** at $x = 0$, T at $x = -5$ mm, (c)-(d) plane *XZ*, **B** at $y = 0$, T at $y = -5$ mm

Figure 8.
Magnetic flux density vectors together with temperature field distribution in the vicinity of the keyhole for HT-MA (a, c) and HT-DC-MA (b, d) analysis

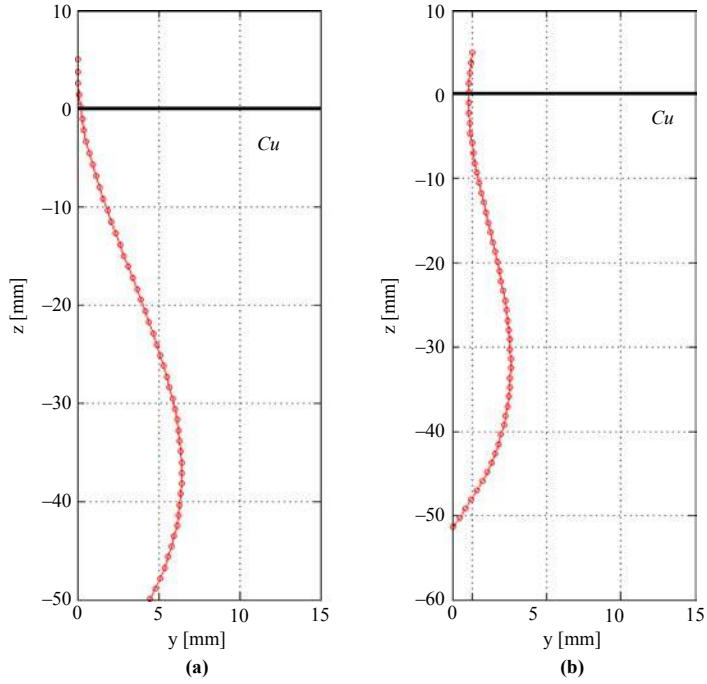

Figure 9.
Trajectory of electron beam for HT-MA analysis (a) tilt angle $\alpha = 0$, (b) tilt angle $\alpha = 5°$

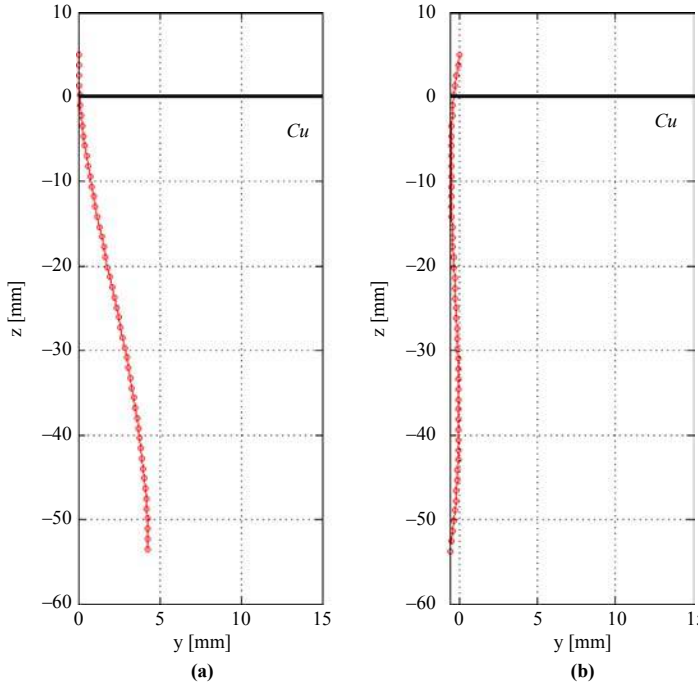

Figure 10.
Trajectory of electron beam for HT-DC-MA analysis (a) tilt angle $\alpha = 0$, (b) tilt angle $\alpha = 5°$

References

Goldak, J.A. and Akhlaghi, M. (2005), *Computational Welding Mechanics*, Springer Science + Business Inc., Heidelberg.

Lide, D.R. (2006), *CRC Handbook of Chemistry and Physics, 2006-2007*, 87th ed., Taylor&Francis, London.

Nazarenko, O.K. (1982), "Deflection of the electron beam in electron-beam welding", *Avt. Svarka*, Vol. 346 No. 1, pp. 33-9.

Paulini, J., Simon, G. and Decker, I. (1990), "Beam deflection in electron beam welding by thermoelectric eddy currents", *J. Phys. D: Appl. Phys.*, Vol. 23, pp. 486-95.

Shercliff, J.A. (1979), "Thermoelectric magnetohydrodynamics", *J. Fluid Mech.*, Vol. 91, pp. 231-51.

Wei, P.S. and Lii, T.W. (1990), "Electron beam deflection when welding dissimilar metals", *Journal of Heat Transfer*, Vol. 112, pp. 714-20.

About the authors

Marek Ziolkowski received MSc and PhD in electrical engineering from the Technical University of Szczecin in 1978 and 1984. Since 1978 he has been working there at the Chair of Theoretical Electrotechnics and Computer Science. Since 2001 he is also with the Technische Universitaet Ilmenau. His main research interests include numerical calculations and visualization of EM fields, biomagnetic problems and inverse problems in magnetic fluid dynamics. Marek Ziolkowski is the corresponding author and can be contacted at: marek.ziolkowski@tu-ilmenau.de

Hartmut Brauer received Diploma Engineer and Dr -Ing. in electrical engineering from the Ilmenau Institute of Technology in 1975 and 1982. Since 1975 he is with the Department of Electromagnetic Fields/Theoretical Electrical Engineering at the Technische Universitaet Ilmenau. His main research interests include computation of electromagnetic fields and inverse field problems/optimization in electrical engineering, with applications to bioelectromagnetics, magnetic fluid dynamics and educational aspects.